

## Inelastic pion scattering from $^{13}\text{C}$ at 65 MeV

J. H. Mitchell,\* J. T. Brack, R. J. Peterson, R. A. Ristinen, and J. L. Ullmann†  
*University of Colorado, Boulder, Colorado 80309*

R. L. Boudrie  
*Los Alamos National Laboratory, Los Alamos, New Mexico 87545*

B. G. Ritchie  
*Arizona State University, Tempe, Arizona 85287*

J. Escalante  
*University of South Carolina, Columbia, South Carolina 29208*  
 (Received 28 September 1987)

Differential cross sections for  $^{13}\text{C}(\pi^\pm, \pi^\pm)^{13}\text{C}^*$  were measured at an incident pion energy of 65 MeV. Data were gathered for several states up to 11.8 MeV in excitation energy. The experimental results are compared to distorted wave impulse approximation calculations and to other pion scattering data from the same nucleus at higher beam energies. The striking enhancement of  $\pi^-$  over  $\pi^+$  scattering to the 9.5 MeV  $\frac{9}{2}^+$  state observed in previous studies at resonance energies is found to persist at 65 MeV.

### I. INTRODUCTION

Due to the availability of pions in three charge states, pion-nucleus scattering data, both elastic and inelastic, provide many unique insights into nuclear structure. However, the full range of information available from this probe has only begun to be explored. In particular, though the meson factories have been in operation since the 1970's, there are very few inelastic scattering data at pion energies below the (3,3) resonance.<sup>1-3</sup> This situation is not due to a lack of interest in the inelastic scattering of low-energy pions but rather to the lack of a spectrometer facility having high resolution and designed for work at subresonant energies. In fact, low-energy pions have some characteristics which make them more desirable as nuclear probes than pions of resonant energy. At low beam energies the fundamental pion-nucleon cross sections are smaller than at resonance and hence the pion-nucleus interaction should be less surface peaked at low energies. The smaller fundamental cross section suggests that the contributions of true absorption and other medium corrections to the optical potential will be more readily observed because at lower energies the angular distributions for elastic and inelastic scattering are not dominated by purely diffractive effects. Thus, for cases where the nuclear structure is known from other measurements, low-energy elastic and inelastic data may be crucial to constrain the descriptions of these medium modifications of the free  $\pi\text{N}$  interaction.

The application of simple isospin relations and the assumption of delta dominance can be used to explain the observed, essentially angle independent, 9 to 1 ratio of  $d\sigma(\pi^+p)/d\sigma(\pi^-p)$  at resonance. This isospin selectivity of the resonant pion-nucleon system has been used to

extract the isospin component of collective transitions by comparison of data obtained with an incident  $\pi^-$  beam to data for the same transitions acquired with a  $\pi^+$  beam.<sup>4</sup> Comparison of the relative strength of excitations in  $\pi^+$  and  $\pi^-$  scattering at energies below the resonance can yield similar information, but here the relative sensitivity of the incoming probe to neutrons and protons is very angle dependent due to interference of the  $s$  and  $p$ -wave amplitudes. At very large angles low-energy negative (positive) pions are practically insensitive to protons (neutrons).<sup>2,3</sup>

The current data for the scattering of both positive and negative pions from  $^{13}\text{C}$  were measured with an average center-of-target energy of 64.7 MeV. This energy was used for several reasons. First, the beam flux is high enough to provide reasonable count rates for pions of either charge. Second, there already exist several sets of elastic scattering data for normalization.<sup>5,6</sup> These previous data have been included in the data base for the fitting of the phenomenological pieces of the optical potential used to describe the medium modifications of the  $\pi\text{N}$  interaction.<sup>7,8</sup> Thus, reasonable values of these parameters exist and the ability of these parameters to describe new data may be investigated. Finally, between 90 and 110 deg, the ratio of  $\pi^+p$  to  $\pi^-p$  cross sections for 65 MeV pions is very close to the 9 to 1 ratio found at resonance. The largest angle at which data were obtained in the current measurements was 105 deg in the laboratory frame. All the transitions of low multipolarity have backward-peaked angular distributions at this energy. If the 65 MeV data are handled in such a way that the back angle data points are given more weight than the forward angle data, the differences in the isospin selectivity of resonant and low-energy pions will at least be partially negated. Therefore, it may be possible to

isolate clearly effects due to the differing radial sensitivities of low-energy and resonant pions.

The  $^{13}\text{C}$  target has a number of well-separated states that are resolvable in a medium resolution study. Therefore  $^{13}\text{C}$  presents an opportunity to examine the inelastic scattering of charged pions to states with a variety of quantum numbers and well-understood structure. Such a study also provides a chance to compare the results of a low-energy experiment with an extensive set of resonant-energy pion scattering data as well as with results obtained from experiments utilizing other probes.<sup>9-13</sup> Such a comparison will help determine whether the theoretical techniques that have proven successful for the interpretation of resonant energy scattering data can also provide a consistent description of the more complicated reaction mechanism at 65 MeV. Coarse angular distributions were obtained for several of the low lying states in  $^{13}\text{C}$ . These transitions are largely collective in nature, although one of them (the  $\frac{3}{2}^+$  state at 9.5 MeV) is believed to have a reasonably pure single-particle structure.<sup>9,14</sup>

## II. EXPERIMENTAL PROCEDURE

The experiment was performed on the Low Energy Pion Channel (LEP) at the Los Alamos Meson Physics Facility (LAMPF). This facility has been described elsewhere.<sup>15,16</sup> The scattered pions were momentum analyzed using the clamshell spectrometer.<sup>17</sup> This device has a short path length (1.8 m), a large solid angle (40 msr), and good momentum resolution (0.4%), making it uniquely qualified for the study of inelastic pion scattering at energies below the (3,3) resonance, where the cross sections and beam fluxes are low and the decay of the pions is important.

The  $^{13}\text{C}$  target has areal density of  $203 \pm 3$  mg/cm<sup>2</sup> and was isotopically enriched to 99 percent. The target was always placed in transmission geometry with the target angle equal to one half the scattering angle.

The pions were detected at the exit of the spectrometer by a counter array consisting of two sets of x-y delay line readout drift chambers followed by two 6.2 mm thick scintillators. The wire chambers are identical to those used at other LAMPF spectrometer facilities and are discussed elsewhere.<sup>18</sup> There were no counters at the entrance to the spectrometer. The target coordinates associated with each event were reconstructed from the information gathered at the focal plane using previously calibrated spectrometer matrix elements.<sup>19</sup>

The missing mass spectra, from which peak areas were extracted, had a resolution of approximately 500 keV full width at half maximum (FWHM) for an incident pion energy of 65 MeV. A sample spectrum for each pion charge state is shown in Fig. 1. The line shape parameters (width and skew) used in the fitting of the inelastic peaks were fixed to be those that best described the elastic peak. The peak separations were fixed by an energy calibration to the tabulated energies of the states.<sup>20</sup> This energy calibration was obtained by fitting the prominent collective excitations in  $^{13}\text{C}$ , and was checked against an independent calibration taken from

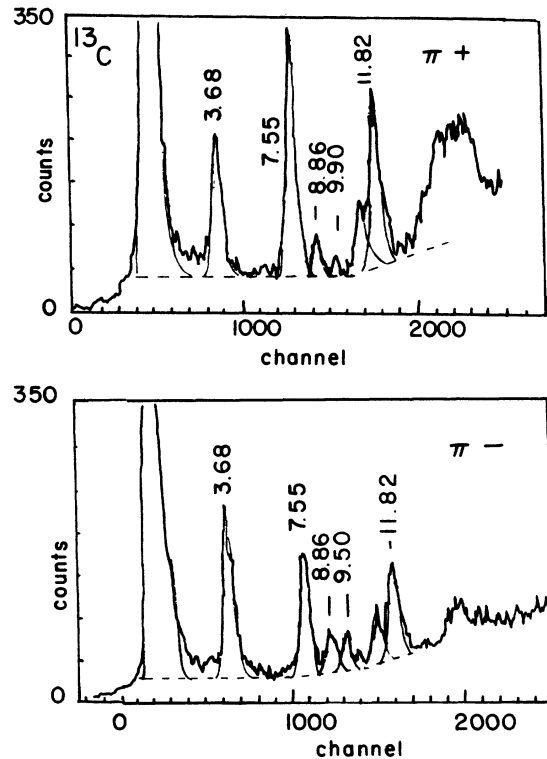


FIG. 1. Representative missing mass spectra for the scattering of both positive and negative pions from  $^{13}\text{C}$ . The data were taken at a lab angle of 105 deg and have a resolution of approximately 510 keV (FWHM).

$^{12}\text{C}$  spectra. The background was assumed to be linear and the effect of the choice of background parameters upon the extracted peak areas was estimated by varying these parameters over reasonable limits. The peak shapes used were unable to account completely for the low energy tail of the peaks; this tail is largely due to Landau straggling in the target. The magnitude of this effect was estimated and a correction for it is included in the final areas.

The beam was monitored using three methods. The first monitor was the primary toroid which integrates the charge in the primary proton beam; the second monitor was an ion chamber that views the spallation products from the pion production target. The final monitors were a pair of plastic scintillator telescopes mounted at the exit of the channel and designed to observe muons resulting from the in-flight decay of pions. At any given scattering angle, the three monitoring methods were found to yield consistent results, since the beam channel settings were held constant. Unfortunately, the results from the in-cave muon counters exhibited an apparent angular variation due to the spectrometer fringe field. For this reason, the data in this paper were normalized by the proton toroid counter; previous experience has shown that the proton toroid is in good agreement with the in-cave counters at the EPICS facility at Los Alamos National Laboratory.<sup>4</sup>

The extracted peak areas were corrected for computer

live time, chamber efficiency and pion decay losses. In addition, the change in the spectrometer acceptance as a function of position on the focal plane was accounted for by tracking a given peak across the focal plane to determine the acceptance.

The final normalization of the acceptance solid angle for the  $^{13}\text{C}(\pi^+, \pi^+)$  reaction was obtained by comparing measured yields for the reaction  $^{12}\text{C}(\pi^+, \pi^+)$  to the elastic scattering cross sections for this same reaction published by Blecher *et al.*<sup>5</sup> The relative normalization of the  $\pi^-$  data was taken from elastic scattering using a  $\text{CD}_2$  target, with comparisons to the  $\pi^\pm d$  data of Balestri *et al.*<sup>6</sup> This normalization was chosen because there was a discrepancy between the normalization factors obtained by comparing the scattering of pions from  $^{12}\text{C}$  to the data of Blecher *et al.* and those obtained by comparing the scattering of pions from carbon and deuterium in the  $\text{CD}_2$  target to the data of Balestri *et al.* This discrepancy (about 20 percent for  $\pi^+$ ) was greater than one would have expected given the statistical uncertainty of the normalization measurements (3 percent) and the errors quoted for the two sets of normalization data. The choice of normalizations does not significantly affect any of the conclusions of this work.

The error bars in all figures represent only the statistical error and that due to an uncertainty in peak fitting. In addition, there is an overall systematic uncertainty of 10 percent for the  $\pi^+$  data and 11 percent for the  $\pi^-$  data. These systematic errors are dominated by the un-

certainties in the several measurements to which the current data were normalized.

### III. RESULTS AND COMPARISON WITH THEORETICAL CALCULATIONS

The measured elastic cross sections for both  $\pi^+$  and  $\pi^-$  scattering are shown in Fig. 2. In addition to the results from the present work, the earlier data of Blecher *et al.*<sup>5</sup> are also shown. The agreement for the scattering of positive pions is good at most angles. This is expected since the data of this work were normalized to these earlier  $^{12}\text{C}$  measurements. The difference between the two sets of  $\pi^-$  data is about 20 percent and is due to the choice of normalization for the present data (as previously discussed).

In addition to the data, the figure shows the results of two sets of optical model calculations. These calculations, as well as those for all the collective excitations, were performed with the code DWPIES,<sup>21</sup> using the potential discussed by Siciliano *et al.*<sup>22</sup> Neglecting correlation and isotensor terms, the first order optical potential is

$$U_{\text{opt}}^1(r) = -k^2[\lambda_{s,0}^1 \rho_0(r) + \lambda_{s,1}^1 \rho_1(r)] \\ + \nabla[\lambda_{p,0}^1 \rho_0(r) + \lambda_{p,1}^1 \rho_1(r)] \nabla \\ - \frac{1}{2} \nabla^2 \{ (p_1 - 1) [\lambda_{p,0}^1 \rho_0(r) + \lambda_{p,1}^1 \rho_1(r)] \} .$$

Similarly, the second order potential is given by

$$U_{\text{opt}}^2(r) = \frac{-k^2}{\rho_{\text{avg}}} \{ \lambda_{s,0}^2 [\rho_0(r)]^2 + \lambda_{s,1}^2 \rho_0(r) \rho_1(r) \} + \frac{1}{\rho_{\text{avg}}} \nabla \{ \lambda_{p,0}^2 [\rho_0(r)]^2 + \lambda_{p,1}^2 \rho_0(r) \rho_1(r) \} \nabla \\ - \frac{1}{2\rho_{\text{avg}}} \nabla^2 \{ (p_2 - 1) \{ \lambda_{p,0}^2 [\rho_0(r)]^2 + \lambda_{p,1}^2 \rho_0(r) \rho_1(r) \} \} .$$

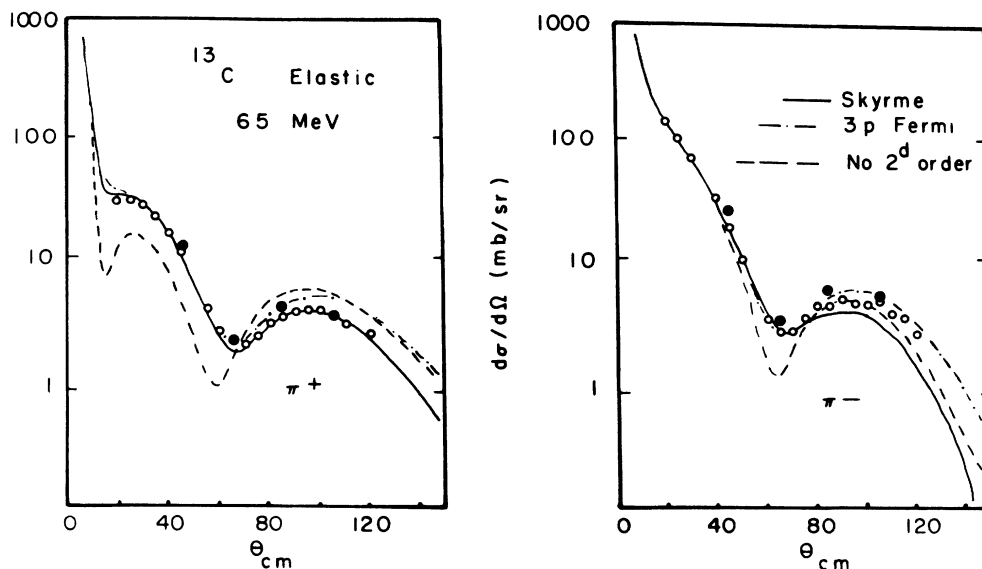


FIG. 2. Data from the present experiment are shown for  $\pi^+$  and  $\pi^-$  elastic scattering at  $T_\pi = 65$  MeV (solid circles). Also shown are the data of Ref. 5 (open circles). The curves are optical model calculations using two different ground state matter distributions and also one which shows the effects of setting the second order parameters to zero.

In these equations the  $\lambda_{1,t}^n$  are the  $n$ th order coupling strengths for the various angular momentum and isospin channels. The first-order coupling strengths were obtained from the *FP85* phase shift solution,<sup>23</sup> while the second-order terms, which describe medium modifications of the interaction, are due to the work of Alons *et al.*<sup>7,8</sup> This is a set of phenomenological parameters that were found to give calculated cross sections that fit a range of pion elastic scattering and single charge exchange data. In the present calculations, only the second-order isoscalar parameters ( $s$  wave and  $p$  wave, real and imaginary) were taken to be nonzero. No isotensor terms were included. In addition, the imaginary parts of the first-order potential were reduced by a momentum-dependent factor (0.392 in the present case) to account for Pauli blocking (according to the prescription of Landau and MacMillan<sup>24</sup>).

For 65 MeV incident pions incident on  $^{13}\text{C}$ , the kinematic factors are

$$p_1 = \frac{(1+\varepsilon)}{(1+\varepsilon/A)} = 1.198, \quad p_2 = \frac{(1+\varepsilon/2)}{(1+\varepsilon/A)} = 1.091,$$

with

$$M_p \varepsilon = (K_\pi^2 + m_\pi^2)^{1/2}.$$

The first-order couplings (in  $\text{fm}^3$ ) are  $\lambda_{s,0}^1 = -1.9698 + 0.2789i$ ,

$$\lambda_{s,1}^1 = -3.9260 + 0.0547i,$$

$$\lambda_{p,0}^1 = 8.2994 + 0.6214i,$$

and

$$\lambda_{p,1}^1 = 4.9022 + 0.3066i.$$

The second order couplings are

$$\lambda_{s,0}^2 = 0.820 - 0.50i \quad \text{and} \quad \lambda_{p,0}^2 = 0.730 + 2.57i.$$

The ground state matter distributions, for both neutrons and protons, used in all the calculations are the results of a self-consistent analysis using a Skyrme-III force,<sup>25,26</sup> chosen because these were used in the work of Alons *et al.*<sup>7,8</sup> The sensitivity of the elastic scattering calculations to the choice of matter distributions was investigated and it was found that at angles beyond the first minimum the effect could be as large as 50 percent.<sup>17</sup> These densities are included as their isoscalar  $\rho_0(r)$  and isovector  $\rho_1(r)$  forms in the potentials above, normalized to their average  $\rho_{\text{avg}}$ .

Where calculations are compared to the data for the three-parameter Fermi distribution as well as for the Skyrme III distributions, both neutron and proton densities are given by

$$\rho(r) = \frac{(1 + wr^2/R^2)}{\{1 + \exp[(r-R)/z]\}^{-1}},$$

with  $R = 2.40$  fm,  $z = 0.41$  fm, and  $w = -0.16$ , as used for  $^{13}\text{C}$  at 162 MeV.<sup>10</sup> Calculations with this distribution are shown only with the full optical model distortions, compared to the data and the Skyrme III calculations for the elastic,  $\Delta L = 0$ ,  $\Delta L = 2$ , and  $\Delta L = 3$  collec-

tive transitions. All inelastic calculations use the same normalizing amplitude  $\beta R$ , determined by the fit with the Skyrme calculations.

Three calculations are shown in Fig. 2. The first uses the potential described in the previous paragraphs, while the second shows the dramatic effect of setting all the second-order (rho-squared) terms in the optical potential to zero. The curves calculated with the second-order terms provide an adequate description of the elastic scattering data for both  $\pi^-$  and  $\pi^+$  incident beams. This is important since this potential will be used to generate the distorted waves for the calculation of inelastic cross sections. Second-order calculations using the three-parameter Fermi distribution are very similar to those using the Skyrme distributions.

The collective states at 3.68 and 7.55 MeV are related to the 4.44 MeV ( $J^\pi = 2^+$ ) state in  $^{12}\text{C}$ . The state at 3.68 MeV has a spin and parity of  $\frac{3}{2}^-$  and was assumed to undergo a  $\Delta L = 2$ ,  $\Delta S = 0$  transition from the ground state in accordance with the collective nature of its structure. The calculated curves (see Fig. 3) utilize a collective transition density which was formed by numerically differentiating the ground state Skyrme or Fermi distribution. The calculated curves for the state at 7.55 MeV ( $J^\pi = \frac{5}{2}^-$ ) also assume a  $\Delta L = 2$ ,  $\Delta S = 0$  transition from the ground state (also in Fig. 3). As for the elastic data, three calculated curves are shown in all the figures of inelastic data. The first curve is the full calculation with the Skyrme distributions. This calculation includes the rho-squared terms in the optical potential used to generate the distorted waves. It should be noted that no medium terms have been included in the interaction that drives the transition. The magnitudes of second-order effects in the transition term have been estimated and were found to be small at large angles for 50 MeV pion scattering to the 4.44 MeV state in  $^{12}\text{C}$ .<sup>27</sup> The second curve shows the effect of turning off these medium terms in the distorting potential and is included to demonstrate the sensitivity of the calculations to the presence of these rho-squared corrections. Calculations using the Fermi density show sensitivity to the assumed nuclear structure at small angles, as the third curve.

The normalization of the calculated angular distributions for all the collective transitions was determined so that the full calculation best fit the high-accuracy back-angle data points and the normalization factor ( $\delta_{lm}^2 = d\sigma/d\Omega_{\text{exp}}/d\sigma/d\Omega_{\text{calc}}$ ) was used to extract deformation lengths,  $\delta_{lm} = \beta_{lm}R$ , used also for the other curves. The errors in the extracted deformation lengths in all cases were determined by an extreme credible fit procedure. The values of the deformation lengths for all the collective states analyzed are summarized in Table I. Also included in the table are the values of these deformation parameters that were extracted from other pion data as well as those found in inelastic proton scattering.<sup>9-13</sup> Before discussing further the quantitative results (deformation lengths), it is useful to make a more qualitative comparison of the theoretical curves and the measured angular distributions for all transitions.

The state at 8.86 MeV has a spin and parity of  $\frac{1}{2}^-$  and its dominant mode of excitation is through a natural

parity  $\Delta S = \Delta L = 0$  transition from the ground state.<sup>28</sup> Hence, the theoretical curves shown utilize a volume-conserving monopole transition density that was obtained from the ground state Skyrme or Fermi densities by a numerical calculation of the quantity

$$\rho_{tr} = 3\rho_{ground} + \frac{r d\rho_{ground}}{dr}.$$

The calculations (see Fig. 4) which include the second-order effects reproduce the minimum in the experimental distribution. It is seen that the position of the minimum is also somewhat sensitive to the exact choice of transition density.

The final collective state that was studied in the  $\frac{5}{2}^+, \frac{7}{2}^+$  doublet at 11.8 MeV in excitation. These states

were assumed to undergo  $\Delta L = 3, \Delta S = 0$  transitions from the ground state. Figure 5 shows the data and the theoretical angular distributions for this peak. The theoretical curves look quite similar, but again the contribution of the rho-squared terms in the distorting potential is significant.

Table I shows the deformation lengths that were extracted from the experimental data as well as the results from similar analyses with different probes and pions of different energies. The deformation lengths presented for the pion experiments performed at higher energies are from Ref. 17 and are discussed in detail there. The present calculations for all the energies were made in a consistent manner in that they all use the Skyrme densities for both the ground state and transition densities

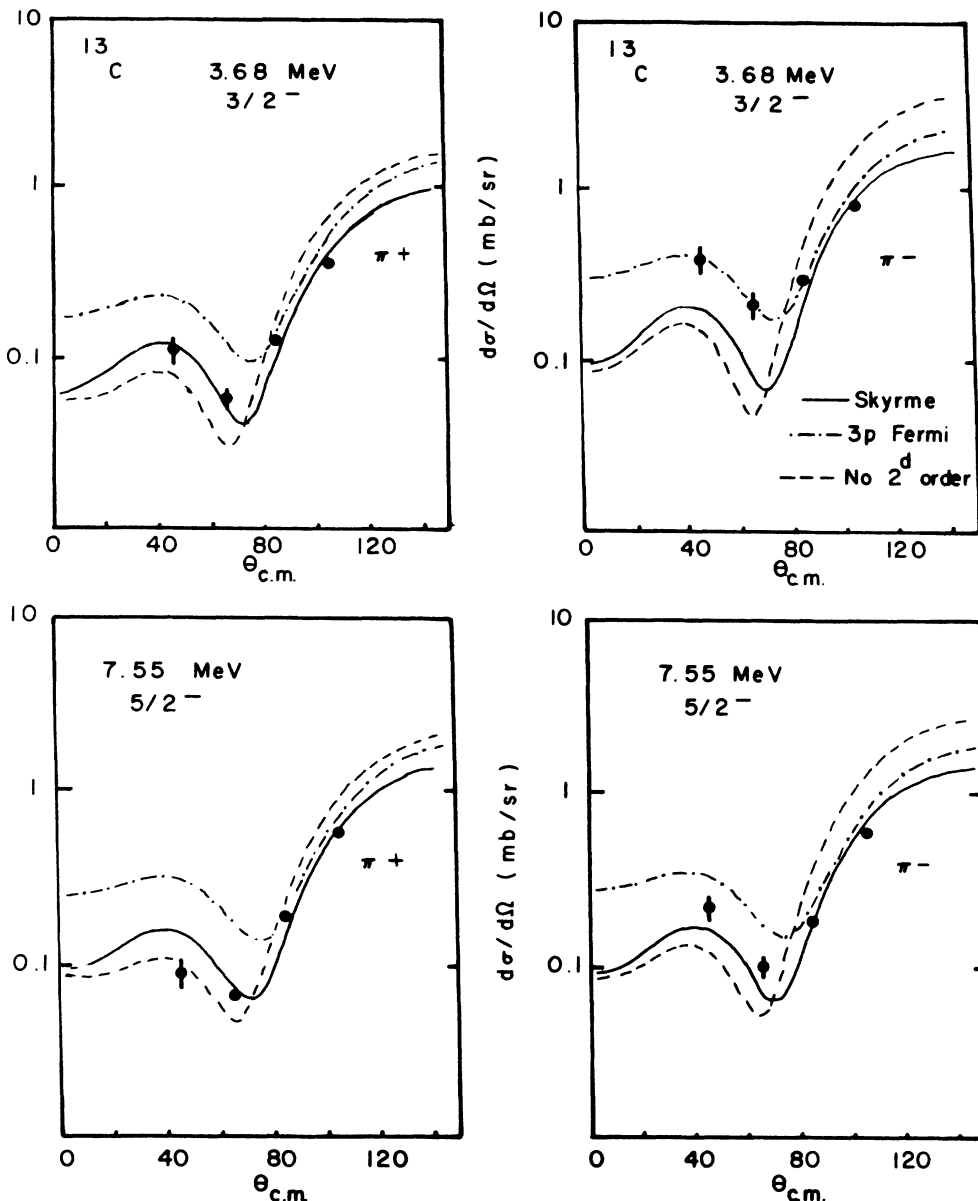


FIG. 3. Data for scattering  $\pi^+$  and  $\pi^-$  to the  $\frac{3}{2}^-$  state at 3.68 MeV and to the  $\frac{5}{2}^-$  state at 7.55 MeV. The curves are the distorted wave calculations discussed in the text.

TABLE I. The extracted deformation lengths  $(\beta R)_{\pm}$  (in fm) for  $\Delta S=0$  collective states of  $^{13}\text{C}$ , from this experiment as well as those from other pion data. Also included are the deformation lengths obtained from the analysis of 800 MeV proton scattering data. The results are discussed in the text. For the  $\frac{1}{2}^{-}$  state the values quoted are  $\beta_{\pm}$  not  $(\beta R)_{\pm}$ .

State (MeV)	3.68	7.55	8.86	11.8
$J^{\pi}$	$\frac{3}{2}^{-}$	$\frac{5}{2}^{-}$	$\frac{1}{2}^{-}$	$\frac{5}{2}^{+}, \frac{7}{2}^{+}$
$\Delta L$	2	2	0	3
$T_{\pi}=65$ MeV (this work)				
$(\beta R)_{+}$	$1.34 \pm 0.11$	$1.30 \pm 0.10$	$0.1 \pm 0.01$	$1.48 \pm 0.13$
$(\beta R)_{-}$	$1.40 \pm 0.25$	$1.10 \pm 0.10$	$0.09 \pm 0.01$	$1.02 \pm 0.07$
$(\beta R)_{\text{avg}}$	$1.37 \pm 0.14$	$1.19 \pm 0.07$	$0.095 \pm 0.01$	$1.23 \pm 0.08$
$(\beta R)_{+}/(\beta R)_{-}$	$0.95 \pm 0.2$	$1.18 \pm 0.12$	$1.11 \pm 0.15$	$1.45 \pm 0.16$
$T_{\pi}=100$ MeV (Ref. 11)				
$(\beta R)_{+}$	$1.92 \pm 0.29$	$1.67 \pm 0.10$		$1.73 \pm 0.29$
$(\beta R)_{-}$	$1.73 \pm 0.43$	$1.30 \pm 0.15$		$1.45 \pm 0.35$
$(\beta R)_{\text{avg}}$	$1.82 \pm 0.27$	$1.47 \pm 0.11$		$1.58 \pm 0.23$
$(\beta R)_{+}/(\beta R)_{-}$	$1.11 \pm 0.3$	$1.28 \pm 0.13$		$1.20 \pm 0.3$
$T_{\pi}=162$ MeV (Ref. 9)				
$(\beta R)_{+}$	$1.48 \pm 0.07$	$1.48 \pm 0.10$	$0.130 \pm 0.008$	$2.12 \pm 0.09$
$(\beta R)_{-}$	$1.41 \pm 0.04$	$1.10 \pm 0.09$	$0.075 \pm 0.01$	$1.84 \pm 0.08$
$(\beta R)_{\text{avg}}$	$1.44 \pm 0.05$	$1.28 \pm 0.07$	$0.10 \pm 0.01$	$1.97 \pm 0.06$
$(\beta R)_{+}/(\beta R)_{-}$	$1.04 \pm 0.05$	$1.34 \pm 0.11$	$1.73 \pm 0.15$	$1.15 \pm 0.06$
$T_{\pi}=180$ MeV (Ref. 10)				
$(\beta R)_{+}/(\beta R)_{-}$	$1.05 \pm 0.05$	$1.16 \pm 0.10$		$1.14 \pm 0.05$
800 MeV ( $p, p'$ ) (Ref. 12)				
$(\beta R)_0$	$1.44 \pm 0.07$	$1.23 \pm 0.06$		$1.32 \pm 0.07$

and they all include second-order terms in the distorting potential. The lengths extracted are given in several ways. First, values of  $(\beta R)_{+}$  and  $(\beta R)_{-}$  are quoted. These are important for it is through a comparison of  $(\beta R)_{+}$  and  $(\beta R)_{-}$  that the isospin character of the transitions can be seen. Second, in an attempt to compare

fairly these data with the results from other probes and energies the quantity  $(\beta R)_{\text{avg}} = [Z(\beta R)_{+} + N(\beta R)_{-}] / A$  is quoted. This is a weighted average of the information obtained from the two pion charges. Other prescriptions for making comparisons exist in the literature but most assume (3,3) dominance of the amplitude. Even though

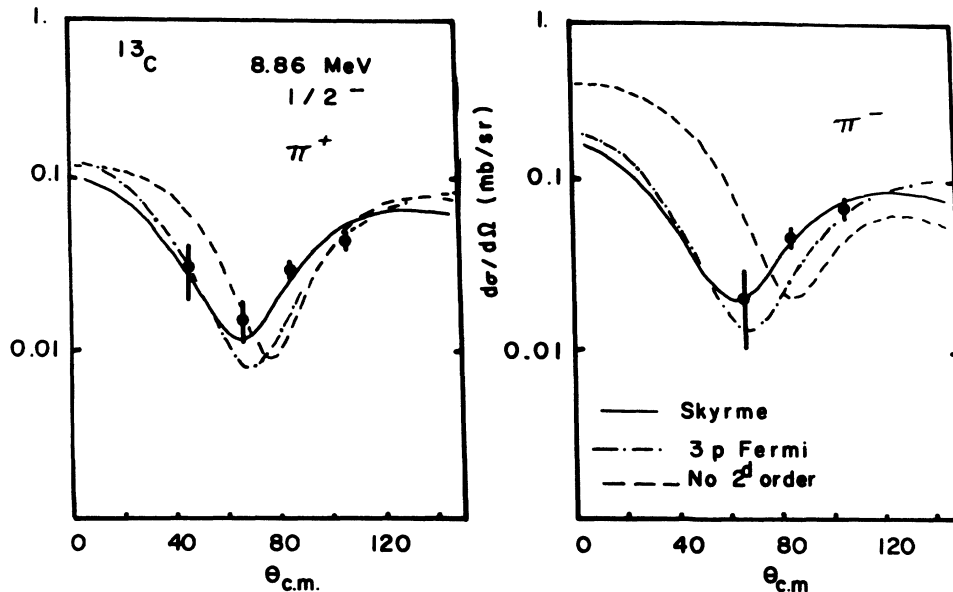


FIG. 4. Data and calculations for  $\pi^{+}$  and  $\pi^{-}$  scattering for the monopole transition at 8.86 MeV. The curves are discussed in the text, but are from the same calculations as shown in Fig. 3.

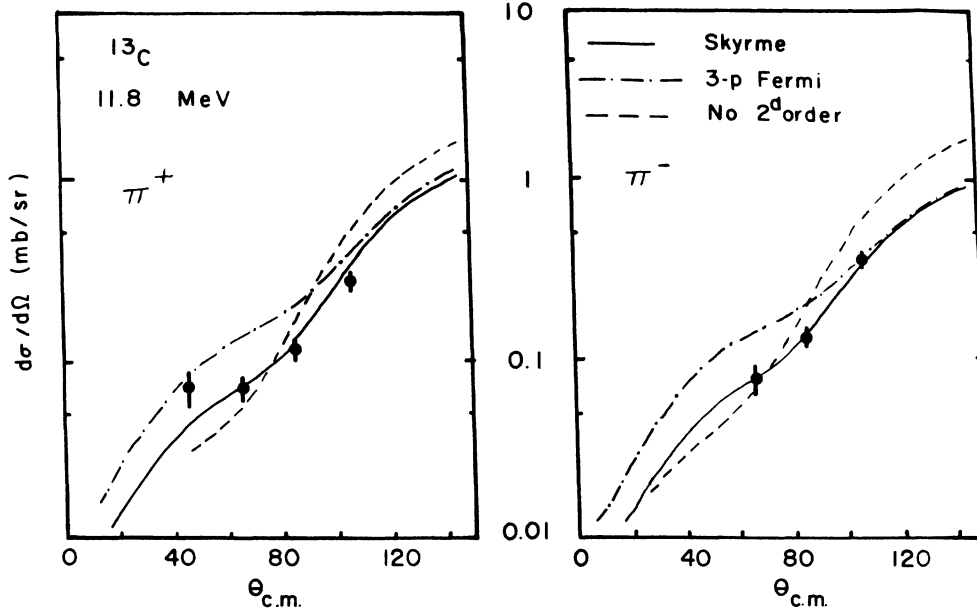


FIG. 5. Measured angular distributions for the scattering of positively and negatively charged pions to the peak at 11.8 MeV. The curves assume that this is a  $\Delta L=3$  transition.

(3,3) dominance does not hold, the isospin sensitivity of 65 MeV pions is approximately the same as that of resonant pions,<sup>2</sup> so any reasonable weighting scheme should be adequate. For  $^{13}\text{C}$  this quantity,  $(\beta R)_{\text{avg}}$ , differs only slightly from the isoscalar deformation length,  $(\beta R)_0$ , as given in Ref. 4 [note that the formula given in this reference which connects the measured  $(\beta R)_-$  and  $(\beta R)_+$  to the isoscalar deformation assumes hydrodynamic collective motion and delta dominance]. The values of the ratios  $(\beta R)_+ / (\beta R)_-$  for the pion experiments at all energies agree (within errors) as to whether a state is more strongly excited by positive or negative pions. Although there is qualitative agreement, the quantitative agreement for the whole range of transitions is less dramatic. For the two lowest collective states (the  $\Delta L=2$  transitions at 3.68 and 7.55 MeV in excitation) the current work at 65 MeV and the 162 MeV measurements of Seestrom-Morris *et al.*<sup>9</sup> are in excellent agreement with each other and with the results obtained from (essentially isoscalar) 800 MeV proton scattering by Blanpied *et al.*<sup>12</sup> The values of deformations for these two states that were extracted from the 100 MeV pion data of Antonuk *et al.*<sup>11</sup> are about 30 percent larger.

The values of  $(\beta)_{\text{avg}}$  obtained from the two LAMPF pion experiments for the state at 8.86 MeV are in good agreement with the value found by Peterson *et al.*<sup>13</sup> from (purely isoscalar) alpha particle scattering. The higher energy pions find this state to be more asymmetric than the low-energy data would indicate. This effect could be due to the different radial sensitivities of pions at resonant and subresonant energies. Suppose that the proton transition density for this state extends to a slightly greater radius than the neutron transition density. The surface peaked pion interaction at 162 MeV would be very sensitive to this while the effect on

low energy pions would be less. Such an effect would be most pronounced for monopole transitions as the transition densities have a node near the nuclear surface. Perhaps more extensive comparisons of low-energy and high-energy scattering to  $\Delta L=0$  transitions would allow for a confirmation of this hypothesis.

Finally, the agreement between the different sets of pion data on the unresolved states at 11.8 MeV is poor. The value  $(\beta R)_{\text{avg}}=1.23\pm 0.08$  measured with 65 MeV pions is in reasonable agreement with the value  $\beta R=1.32\pm 0.07$  established from 800 MeV proton data.<sup>12</sup> The isospin-averaged value of the deformation obtained from 100 MeV pion data<sup>11</sup> is 30 percent higher than that extracted from the current 65 MeV data. The most interesting point is that in contrast with the results for the other collective excitations, the deformation lengths at 65 and 162 MeV are not in good agreement for this excitation. In addition, the low-energy data also exhibit a larger  $\pi^+ / \pi^-$  asymmetry for this peak than do the data from the higher energy experiments.

The isospin-averaged deformations,  $(\beta R)_{\text{avg}}$ , extracted by comparing the current data at 65 MeV to distorted wave calculations, which include medium corrections (second-order terms in the distorting potential), are in good agreement with the values of the deformations obtained from the inelastic scattering of protons at 800 MeV.<sup>12</sup> If the medium effects are turned off by setting the second-order coupling strengths to zero, the extracted deformation lengths at 65 MeV would all be decreased by 20–40 percent.

In addition to the collective excitations previously discussed, the current data include an angular distribution for the scattering of negative pions to the  $\frac{9}{2}^+$  state at 9.5 MeV in excitation, seen in Fig. 6. This state has been characterized as a very pure neutronlike spin-flip excita-

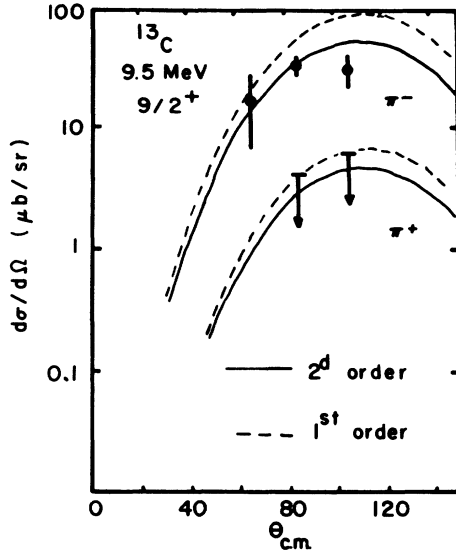


FIG. 6. Measured  $\pi^-$  cross sections and upper limits for  $\pi^+$  scattering to the  $\frac{9}{2}^+$  state. The curves are absolutely normalized distorted wave calculations. The dashed curves have the second-order terms set to zero, while the solid curves include these terms in the distortions.

tion.<sup>9,14,28,29</sup> The experimental data for the scattering of 65 MeV negative pions consist of three angular points which are near the expected peak of the angular distribution. Data were also taken at the same angles for the scattering of positive pions, but due to the exceedingly small cross section for  $\pi^+$  scattering to this state only upper limits (corresponding to 70 percent certainty) can be presented at two angles. The data are compared with microscopic distorted wave calculations performed with the scattering codes ALLWRLD and MSUDWPIES.<sup>30</sup> The calculations use the same distorting potential described previously but the transition term assumes that this excitation has the quantum numbers  $\Delta S=1$ ,  $\Delta L=3$ ,  $\Delta J=4$  (i.e., that it is a pure spin-flip), and hence uses a spin-flip force whose strength was determined from free nucleon phase shifts (in this case from the FP85 solution<sup>23</sup>). The single-particle matrix elements or  $Z$  coefficients were taken from the work of Hicks *et al.*<sup>14</sup> These values are  $Z_0=0.27$  and  $Z_1=0.28$ . Figure 6 shows the data and the calculations. The magnitude of the  $\pi^-$  data is well accounted for by the calculation which includes the second-order terms in the distortions. This is interesting as it indicates that an impulse treatment of the spin-dependent part of the interaction may be sufficient even at these low energies. The upper limits for the  $\pi^+$  data are consistent with the calculated magnitudes and indicate that the asymmetry is at least as large as observed at resonance.<sup>9</sup>

#### IV. SUMMARY AND CONCLUSIONS

This work represents the first study of inelastic pion scattering from  $^{13}\text{C}$  at energies well below the (3,3) reso-

nance. Coarse angular distributions were measured for the collective excitations at 3.68, 7.55, and 11.8 MeV. In addition, data were obtained for pion scattering to the monopole transition at 8.86 MeV in excitation as well as to the spin-flip state at 9.5 MeV. These low-energy data in conjunction with previous higher energy data were used to examine the energy dependence of the pion-nucleus reaction mechanism.

These data were compared to distorted wave calculations and deformation lengths were extracted for the collective excitations. The isospin-averaged deformation lengths obtained from the current data are in good agreement with those obtained from 800 MeV proton scattering<sup>12</sup> and, for the states at 3.68, 7.55, and 8.86 MeV, are in reasonable agreement with those obtained at resonance by Seestrom-Morris *et al.*<sup>9</sup> Further, the deformation lengths found from the 100 MeV pion scattering data of Antonuk *et al.*<sup>11</sup> can be brought into agreement with those found at 65 MeV if a 30 percent renormalization of those results is made. This general agreement indicates that the assumed single-step reaction mechanism is correct for these three excitations. The inclusion of phenomenological terms to account for the medium modification of the free interaction is very important for obtaining this observed agreement. The second-order terms of Alons *et al.*<sup>7,8</sup> seem to give a reasonable description of the contribution of these medium modifications to the distorting potential. A larger data set and calculations which have a more completely constrained nuclear structure contribution (either microscopic shell model transition densities or densities obtained from model independent analysis of electron scattering data) would provide a more stringent test of these parameters. The pion data at different energies do not give consistent transition strengths for the peak at 11.8 MeV. This could be due to the uncertain structure of this multiplet but the discrepancy in the data is not well understood.

The data for the scattering of negatively charged pions to the single-neutron particle-hole state at 9.5 MeV can be adequately described by using a completely constrained microscopic calculation. The experimental upper limits for the scattering of positive pions to this state are consistent with the results of a similar calculation. This agreement is accomplished only by the inclusion of the phenomenological second-order potential of Alons *et al.*<sup>7,8</sup> It appears that a consistent, although phenomenological, picture of pion inelastic scattering to most of the well-known low-lying states in  $^{13}\text{C}$  is possible within the context of existing models.

#### ACKNOWLEDGMENTS

We thank E. R. Siciliano and J. Carr for the use of their computer codes and C. L. Morris for providing the  $^{13}\text{C}$  target. This work was supported in part by the U.S. Department of Energy and the National Science Foundation.



- \*Present address: Vrije Universiteit, Amsterdam, The Netherlands.
- †Present address: Los Alamos National Laboratory, P3 MS D449, Los Alamos, NM 87545.
- <sup>1</sup>S. A. Dytman, J. F. Amann, P.D. Barnes, J. N. Craig, K. G. Doss, R. A. Eisenstein, J. D. Sherman, W. R. Wharton, G. R. Burlison, S. L. Verbeck, R. J. Peterson, and H. A. Thiessen, *Phys. Rev. C* **19**, 971 (1976).
- <sup>2</sup>R. Tacik, K. L. Erdman, R. R. Johnson, H. W. Roser, D. R. Gill, E. W. Blackmore, R. J. Sobie, T. E. Drake, S. Martin, and C. A. Wiedner, *Phys. Rev. Lett.* **52**, 1276 (1984).
- <sup>3</sup>U. Wienands, N. Hessey, B. M. Barnett, F. M. Rozon, A. Altman, R. R. Johnson, D. R. Gill, G. R. Smith, C. A. Wiedner, D. M. Manley, B. L. Berman, H. J. Crawford, and N. Grion, *Phys. Rev. C* **35**, 708 (1986).
- <sup>4</sup>J. L. Ullmann, P. W. F. Alons, B. L. Clausen, J. J. Kraushaar, J. H. Mitchell, R. J. Peterson, R. A. Ristinen, R. L. Boudrie, N. S. P. King, C. L. Morris, J. N. Knudson, and E. F. Gibson, *Phys. Rev. C* **35**, 1099 (1987).
- <sup>5</sup>M. Blecher, K. Gotow, R. L. Burman, M. V. Hynes, M. J. Leitch, N. S. Chant, L. Rees, P. G. Roos, F. E. Bertrand, E. E. Gross, F. E. Obenshain, T. P. Sjoreen, G. S. Blanpied, B. M. Freedom, and B. G. Ritchie, *Phys. Rev. C* **28**, 2033 (1983).
- <sup>6</sup>B. Balestri, G. Fournier, A. Gerard, J. Miller, J. Morgenstern, J. Picard, B. Saghai, P. Vernin, P. Y. Bertin, B. Coupat, E. W. A. Lingeman, and K. K. Seth, *Nucl. Phys.* **A392**, 217 (1983).
- <sup>7</sup>P. W. F. Alons *et al.*, private communication.
- <sup>8</sup>P. W. F. Alons, E. R. Siciliano, and M. J. Leitch, Technical Progress Report, University of Colorado Nuclear Physics Laboratory, 1985 (unpublished).
- <sup>9</sup>S. Seestrom-Morris, D. Dehnhard, M. A. Franey, G. S. Kyle, C. L. Morris, R. L. Boudrie, J. Piffaretti, and H. A. Thiessen, *Phys. Rev. C* **26**, 594 (1982).
- <sup>10</sup>E. Schwarz, J. P. Egger, F. Goetz, P. Gretillat, C. Lunke, C. Perrin, B. M. Freedom, and R. E. Mischke, *Phys. Rev. Lett.* **43**, 1578 (1979).
- <sup>11</sup>L. E. Antonuk, D. Bovet, E. Bovet, J. P. Egger, J. F. Germond, F. Goetz, P. Gretillat, C. Lunke, E. Schwarz, K. Masutani, and T. Takaki, *Nucl. Phys.* **A420**, 435 (1984).
- <sup>12</sup>G. S. Blanpied, W. R. Coker, R. P. Liljestrand, G. W. Hoffman, L. Ray, D. Madland, C. L. Morris, J. C. Pratt, J. E. Spencer, H. A. Thiessen, T. Kozlowski, N. M. Hintz, G. S. Kyle, M. A. Oothoudt, T. S. Bauer, G. Igo, R. J. Ridge, C. A. Whitten, P. M. Lang, H. Nann, and K. K. Seth, *Phys. Rev. C* **18**, 1436 (1978).
- <sup>13</sup>R. J. Peterson, J. R. Shepard, and R. A. Emigh, *Phys. Rev. C* **24**, 826 (1981).
- <sup>14</sup>R. S. Hicks, R. A. Lindgren, M. A. Plum, G. A. Peterson, H. Crannell, D. I. Sober, H. A. Thiessen, and D. J. Millener, *Phys. Rev. C* **34**, 1161 (1986).
- <sup>15</sup>LAMPF Users Handbook, Los Alamos Publication MP-DO-3-UHB.
- <sup>16</sup>R. L. Burman, R. L. Fulton, and M. Jakobson, *Nucl. Instrum. Methods* **131**, 29 (1975).
- <sup>17</sup>J. H. Mitchell, Ph.D. thesis, University of Colorado at Boulder (1987).
- <sup>18</sup>C. L. Morris, *Nucl. Instrum. Methods* **196**, 263 (1982).
- <sup>19</sup>R. L. Boudrie, J. F. Amann, C. L. Morris, H. A. Thiessen, and L. E. Smith, *IEEE Trans. Nucl. Sci.* **NS-26**, 4588 (1979).
- <sup>20</sup>F. Ajzenberg-Selove, *Nucl. Phys.* **A360**, 32 (1981).
- <sup>21</sup>E. R. Siciliano *et al.*, Computer code DWPIES (unpublished).
- <sup>22</sup>E. R. Siciliano, M. D. Cooper, M. B. Johnson, and M. J. Leitch, *Phys. Rev. C* **34**, 267 (1986).
- <sup>23</sup>R. Arndt and L. Roper, Program SAID (unpublished).
- <sup>24</sup>R. Landau and M. McMillan, *Phys. Rev. C* **8**, 2094 (1973).
- <sup>25</sup>T. Skyrme, *Nucl. Phys.* **9**, 615 (1959).
- <sup>26</sup>M. Beiner, H. Flocard, Nguyen Van Giai, and P. Quentin, *Nucl. Phys.* **A238**, 29 (1975).
- <sup>27</sup>K. Stricker, H. McManus, and J. Carr, *Phys. Rev. C* **19**, 929 (1979).
- <sup>28</sup>S. J. Seestrom-Morris, M. A. Franey, D. Dehnhard, D. B. Holtkamp, R. L. Boudrie, J. F. Amann, G. C. Idzorek, and C. A. Goulding, *Phys. Rev. C* **30**, 270 (1984).
- <sup>29</sup>T. Lee and D. Kurath, *Phys. Rev. C* **22**, 1676 (1980).
- <sup>30</sup>J. Carr, computer codes MSUDWPIES and ALLWRLD (unpublished).